

# GFLOW and WhAEM Solver Verifications

H.M. Haitjema



# Contents

<b>1</b>	<b>CODE VERIFICATIONS</b>	<b>5</b>
1.1	WELL IN A UNIFORM FLOW . . . . .	8
1.1.1	Residence times . . . . .	9
1.2	SINK OR SOURCE DISC . . . . .	12
1.2.1	Heads . . . . .	13
1.2.2	Streamline depth . . . . .	13
1.2.3	Residence times . . . . .	15
1.2.4	Superimposed discs . . . . .	18
1.2.5	Top and bottom strengths . . . . .	19
1.3	LINE SINK . . . . .	23
1.4	INHOMOGENEITY DOMAINS . . . . .	29
1.4.1	Discontinuity in hydraulic conductivity . . . . .	29
1.4.2	Discontinuity in recharge . . . . .	35
1.4.3	Discontinuity in porosity . . . . .	41
1.4.4	Residence times . . . . .	41
1.5	COMPARING LINE SINKS WITH AREAL ELEMENTS . . . .	43
1.6	STREAM FLOW ACCUMULATION . . . . .	43
1.7	STREAM FLOW VARIATIONS DUE TO A NEARBY WELL .	43
1.8	CONJUNCTIVE SURFACE WATER / GROUNDWATER SO- LUTIONS . . . . .	43



# Chapter 1

## CODE VERIFICATIONS

The verification of a computer model for groundwater flow may be broken up into two steps:

1. Verification of the accuracy and adequacy of the mathematical (numerical) algorithms used by the program.
2. Verification of the proper *implementation* of these algorithms in the computer code.

The first verification can be carried out without possession of the actual computer code. It entails a theoretical review of the correctness of the mathematical expressions and the adequacy of these algorithms for the intended conceptual models of groundwater flow. Most groundwater flow models are based on well known mathematical principles and use well documented computational procedures to solve the *governing equations* of flow subject to the *boundary conditions* and, for transient flow, *initial conditions* of the problem at hand. Classical solution procedures are: the finite difference method, the finite element method, and the boundary element method. Each of these methods have a variety of variants, most of which have been described in the scientific literature and thus received peer review. Both GFLOW and WhAEM are using the GFLOW1 Solver which is based on the *analytic element method* a contemporary variant of the classical boundary element method. Its development and application were first published by Strack and Haitjema (1981). A complete treatise of the method and its implementation in groundwater flow models is contained in the books *Groundwater Mechanics*, by O.D.L. Strack (1989) and *Analytic Element Modeling of Groundwater Flow*, by H.M. Haitjema (1995). Step 1, the validity of the analytic element method, is not being addressed in this document; it is assumed based on more than 25 years of peer review.

The second task, verification of the *implementation* of the analytic element method in GFLOW or WhAEM, is the subject of the validation problems presented below. Each of these problems has been selected to verify one or more crucial aspect of the operation of these . Although this set of validation problems is believed to ensure proper program operation under most conditions, it

is virtually impossible to guarantee this for *all possible* combinations of model input data. Consequently, the user must always remain alert to improbable solutions.

### Comparison with field data

Testing the integrity of a computer model is carried out by verifying that the program properly represents the **conceptual models** which it is designed to solve. Whether or not these conceptual models are adequate representations of the real world is not the subject of program *verification*! A proper choice of conceptual model, which adequately represents the essential characteristics of a groundwater flow problem, is the responsibility of the modeler. Errors resulting from improper conceptual models often outweigh any numerical inaccuracies, or indeed errors in the computer code. Consequently, comparing model results with field observations is not a proper *computer code verification* procedure, as it is uncertain whether discrepancies are due to code deficiencies or the result of differences between conceptual model and the real world. On the other hand, once a computer code is verified, comparisons with field observations provide valuable insight in the “field performance” of the model. It is important to realize, however, that such field performance may be more dependent on the skills (hydrological insight) of the modeler than on the capabilities of the modeling software.

### The calculation of $Q_i$ , $q_i$ , and $v_i$ in GFLOW1

The computation of the discharge vector  $Q_i$  ( $i = 1, 2$ ) in GFLOW1 is carried out by superimposing the analytical derivatives of the discharge potential  $\Phi$ . Hence, every analytic element in GFLOW1 has both a potential function and a “discharge function” or “derivative function”. The discharge vector at any point in the flow domain is obtained by superimposing all (several hundred perhaps) of the individual derivative functions for the analytic elements in the model. This procedure provides for very accurate discharge calculations, particularly when compared to the numerical derivatives employed by the finite difference codes (e.g. MODFLOW). However, this is also a possible source for code errors. To ensure that the discharge vector calculations are consistent with the calculations of the discharge potential, the latter may be differentiated numerically (like in finite difference models) and compared to the analytic derivative. This will not lead to a perfect match, as the numerical derivative will depend on the stepsize! The user needs to experiment with different stepsizes in order to get a reasonable match between the analytic and numerical derivative. If no satisfactory match can be obtained it may indicate an error in the code.

The discharge vector  $Q_i$  forms the bases for the computation of the specific discharge  $q_i$  and the average groundwater flow velocity  $v_i$ . Consequently, the accuracy of both these vectors depends on the accuracy of  $Q_i$ .

**Incorrect use**

In practice, most model errors are due to incorrect *use* of the model, rather than errors in the computer code. For instance, in GFLOW1 the user is allowed to define stream sections which will be combined into stream networks by the program. In creating these stream networks GFLOW1 relies on consistent stream data and proper stream definitions. If the user forgets to specify an isolated stream section as an “end stream”, GFLOW1 will link it to the nearest stream with a lower head, causing unpredictable results. Similarly, if a tributary to a stream has a lower head than the stream segment to which it is supposed to be linked, GFLOW1 will link it to some other stream segment that happens to have a head lower than the tributary. To the user it may seem, at first, that the program fails to construct a proper stream network, while input data errors are really to blame. Careful verification of input data integrity and critical evaluation of model predictions are the most effective quality assurance measures the user can take.

## 1.1 WELL IN A UNIFORM FLOW

The elementary analytic solution for a well in a uniform flow field allows the computation of some characteristic dimensions of the well's capture zone. It follows from simple continuity of flow considerations that the capture zone width of the well will approach the value  $Q/Q_0$ , where  $Q$  is the pumping rate of the well and where  $Q_0$  is the regional uniform flow rate. In Figure 1.1 a flow net is produced for a well in a uniform flow with by switching the file `valid1.dat` into GFLOW1. The contents of that file is listed below.

```
error error.log
yes
message nul
echo con
quit
title valid1
aquifer
perm 10
thick 10
por 0.2
reference 0 0 100
uniflow 1 0
quit
well
disch
0 0 50 1 *testwell
quit
solve
grid
wind -200 -25 25 25
*wind -10 -12.5 7.957 12.5
horizontalpoints 80
plot flownet
dotmap off
go
quit
switch
mess con
error con
echo input.log
yes
input con
```

The height of the diagram in Figure 1.1 is the width of the domain being plotted and is equal to 50. This width has been chosen equal to the ultimate capture zone width,  $Q/Q_0 = 50/1 = 50$ , as may be observed from the figure.



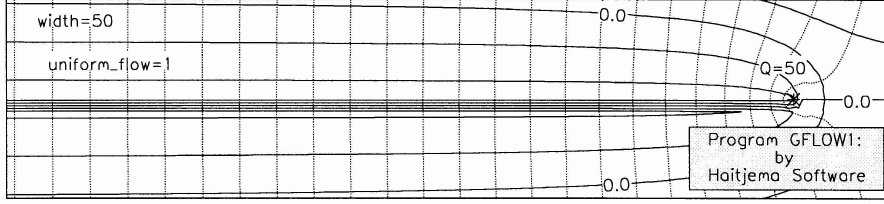


Figure 1.1: Flownet for a well in a uniform flow field. The plotted domain width equals the theoretical ultimate capture zone width.

It can be shown that the capture zone width opposite the well is equal to  $Q/2Q_0$  (Haitjema, 1995), which is 25 with the data in the file `valid1.dat`. The distance  $x_s$  between the well and the stagnation point downstream from the well is given by (Strack, 1989),

$$x_s = \frac{Q}{2\pi Q_0} \quad (1.1)$$

which yields  $x_s = 7.957$  with the same data. In Figure 1.2 a close-up is plotted of the flownet in Figure 1.1. The width of the domain (height of the plot) has been selected equal to 25, while the right-hand boundary of the domain has been chosen exactly equal to 7.957. As may be seen from Figure 1.2 the capture zone width opposite the well is indeed 25, because the bounding streamlines intersect the plot boundaries opposite the well. The stagnation point falls precisely at the right-hand plot boundary: at a distance 7.957 from the well.

### 1.1.1 Residence times

The residence time  $t$  for a water particle, traveling along a streamline, may be calculated as follows:

$$t - t_0 = \int_0^s \frac{ds}{v_s} \quad (1.2)$$

where  $v_s$  is the average groundwater flow velocity along the streamline. The groundwater flow velocity  $v_s$  follows from

$$v_s = \frac{Q_s}{nH} \quad (1.3)$$

where  $Q_s$ ,  $n$ , and  $H$  are groundwater discharge, porosity and aquifer thickness, respectively. When calculating the residence time of a groundwater particle that moves along the horizontal symmetry line through the well (along the negative  $x$ -axis) the integral in (1.2) becomes with (1.3):

$$t = \int_{x_0}^x \frac{nH dx}{Q_x} \quad (1.4)$$

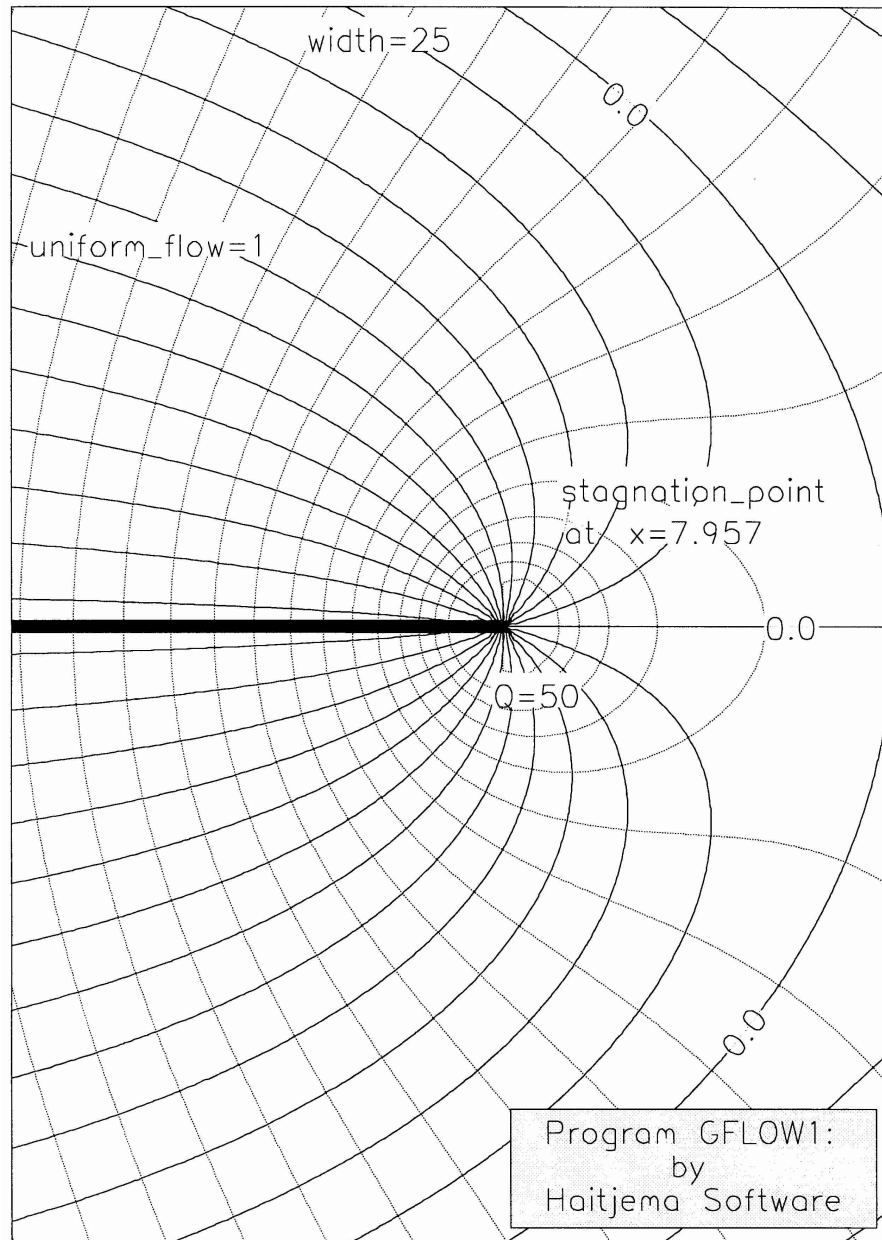


Figure 1.2: Close-up of flownet near the well. The bounding streamlines opposite the well have the same width as the plotted domain (25), while the stagnation point falls on the right-hand domain boundary: at a distance of 7.957 from the well.

where  $Q_x$  is given by, see Strack (1989):

$$Q_x = Q_0 + \frac{Q}{2\pi} \frac{1}{x} \quad (1.5)$$

The residence time for a water particle starting at  $x_0$  and ending at the well follows from:

$$t = \int_{x_0}^{r_w} \frac{nH dx}{Q_0 + \frac{Q}{2\pi} \frac{1}{x}} \quad (1.6)$$

For a streamline starting at the left-hand boundary of Figure 1.1 equation (1.6) has to be integrated between  $x = -200$  and  $x = -1$ , which yields

$$t = \frac{nH}{Q_0} [x - x_s \ln(x + x_s)]_1^{200} \quad (1.7)$$

where  $x_s$  is the distance between the well and the stagnation point to the right of the well as given by (1.1). With the data given in `valid1.dat` the integral yields:

$$t = 2(x - 7.957 \ln(x + 7.957))_1^{200} = 315.0617 - (-32.89) = 347.95$$

We may verify GFLOW1's residence time calculations for this case by switching in the file `valid1.dat` and entering the TRACE module. Use the POINTS command to select the streamline starting point `-20000` and proceed to the graphics screen in TRACE. After streamline tracing stops the program reports a residence time of 347.9 above the plot.

## 1.2 SINK OR SOURCE DISC

The performance of a source disc in GFLOW1 is compared to manual calculations using its analytic solution. This validation checks the *implementation* of this function in GFLOW1.

The data for this problem are contained in the file `valid2.dat`:

```
* Written by GFLOW1 version 1.0
error error.log
yes
message nul
echo con
quit
modelorigin      0      0  0
layout
window -200.0000  -200.0000  200.0000  200.0000
quit
title valid2.dat
aquifer
permeability  10.00000
thickness     10.00000
base          0.0000000
porosity      0.2000000
reference     0.0000    100.00000    100.0000
quit
sinkdisc
discharge
*  x   y   xr   yr   top disch.  bottom disch.  label
   0   0  100   0    -1         0.0         testdisc
quit
solve
grid
dotmap off
horizontalpoints 60
go
quit
switch
error con
message con
echo off
input con
```

Table 1.1: Streamlines and residence times with stepsize 4

starting x,y,z	end x,y,z	residence time
-10 ; + 0 ; +10	-203.0 ; +0.000 ; +0.1071	15.47
+20 ; + 0 ; +10	-203.0 ; +0.000 ; +0.4114	12.62
+0 ; +50 ; +10	+0.000 ; +201.2 ; +2.55	8.873
+0 ; -80 ; +10	+0.000 ; -203.7 ; +6.187	7.188

### 1.2.1 Heads

The head  $\phi_c$  at the center of the disc is calculated from:

$$\phi_c = -\frac{s}{4kH}(r^2 - R^2) + \phi_0 = -\frac{-1}{4.10.10}(0^2 - 100^2) + 100 = 125.0 \quad (1.8)$$

where  $s$  is the strength of the sink disc,  $R$  is the radius of the disc, and  $\phi_0$  is the head at the rim of the disc. The factor  $kH$  is the aquifer transmissivity. GFLOW1 reports the exact same head (125.0) at the center of the disc, which may be verified by switching `valid2.dat` into GFLOW1 and issuing the command “head 0 0” from the main program menu.

### 1.2.2 Streamline depth

The streamline depth underneath the disc may be calculated by use of, see Strack (1984):

$$\mu_{(s)} = e^{-f(s)}\mu_0 \quad (1.9)$$

where  $\mu_{(s)}$  and  $\mu_{(0)}$  are the elevations of points on the streamline at a point  $s$  and a starting point  $s_0$  on the streamline, respectively. The function  $f(s)$  is defined as:

$$f(s) = \int_0^s \frac{N}{Q_s} ds \quad (1.10)$$

where  $N$  is the recharge rate,  $Q_s$  the discharge, and where  $s$  is the distance traveled along the streamline. Note, do not confuse the coordinate  $s$  in (1.9) and (1.10) with the sink disc strength  $s$ ! For the case of the sink disc,  $N$  is replaced by  $-s$  and the coordinate  $s$  along the streamline becomes the radial coordinate  $r$ :

$$f(r) = \int_{r_1}^{r_2} \frac{-s}{-sr/2} dr = 2 \ln \frac{r_2}{r_1} \quad (1.11)$$

In Figure 1.3 four stream lines have been started from the aquifer top inside the rim of the disc. In the table below the starting points, end points, and residence times are given as reported by GFLOW1 using the default stepsize of 4. You may verify these data by switching in `valid2.dat`, entering TRACE, giving the POINTS command and entering the starting points listed in Table 1.1, (optionally set contour on), and press < F2 > until you are in the graphics

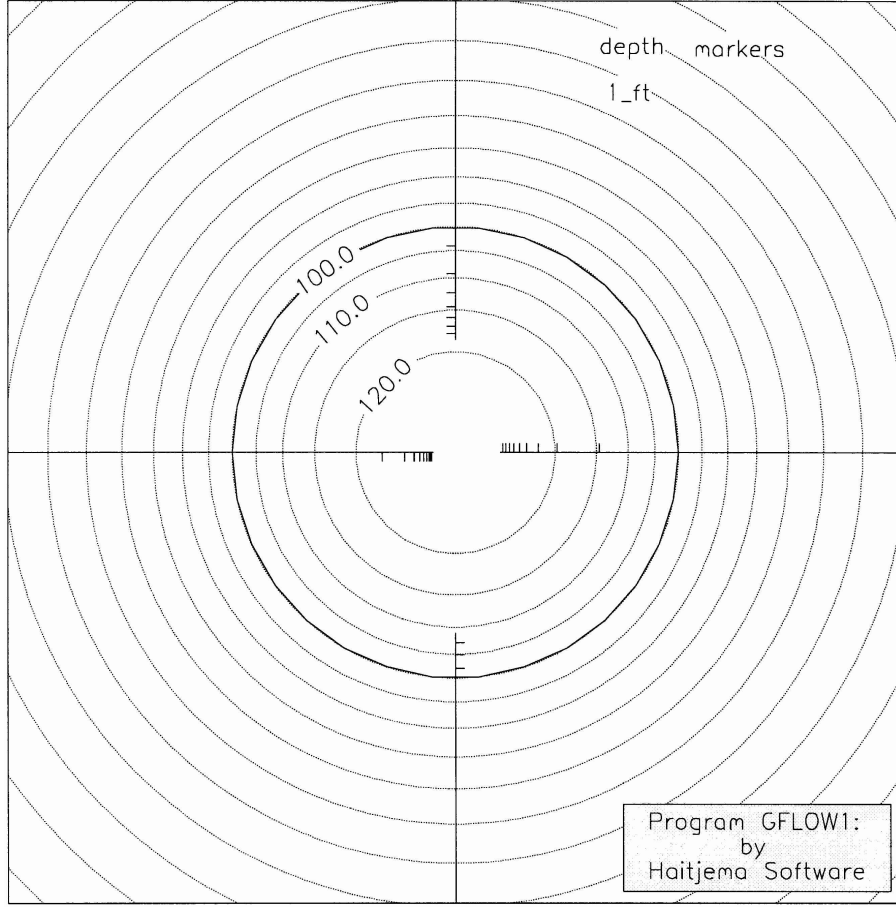


Figure 1.3: Piezometric contours and streamlines with *depth* markers for a source disc.

environment. After the first streamline is completed the data for that streamline is displayed above the plot. By pressing *< Enter >* the next streamline is drawn and the data overwritten by the data for the new streamline.

The vertical movement of a water particle stops as soon as the particle leaves the source disc. Consequently, the value for  $r_2$  in (1.11) is always 100. The value for  $r_1$  varies between 10 and 80. Substituting these values in (1.9) with (1.11) yields for the end elevations  $z_1$  through  $z_2$  of the four streamlines:

$$\begin{aligned}
 z_1 &= e^{-2 \ln(r_2/r_1)} H = e^{-2 \ln(100/10)} 10 = 0.1000 \\
 z_2 &= e^{-2 \ln(r_2/r_1)} H = e^{-2 \ln(100/20)} 10 = 0.4000 \\
 z_1 &= e^{-2 \ln(r_2/r_1)} H = e^{-2 \ln(100/50)} 10 = 2.5000 \\
 z_1 &= e^{-2 \ln(r_2/r_1)} H = e^{-2 \ln(100/80)} 10 = 6.400
 \end{aligned}$$

Table 1.2: Streamlines and residence times with stepsize 1

starting x,y,z	end x,y,z	residence time
-10 ; + 0 ; +10	-200.9 ; +0.000 ; +0.09956	15.28
+20 ; + 0 ; +10	-200.2 ; +0.000 ; +0.4033	12.45
+0 ; +50 ; +10	+0.000 ; +200.2 ; +2.514	8.792
+0 ; -80 ; +10	+0.000 ; -200.7 ; +6.378	6.946

where  $\mu_{(s)}$  has been replaced by  $z_1$  through  $z_4$  and where  $\mu_0$  has been replaced by the aquifer top  $H$ . The  $z$  values must be compared to the end point  $z$  values in the table: 0.1071, 0.4114, 2.55, and 6.187, respectively. The errors in  $z_1$  through  $z_4$  are: 7.1%, 2.8%, 2%, and 3.3%, respectively. These discrepancies are due to the numerical integration of the velocity vector  $v_z$  in GFLOW1. The results may be improved by using a smaller integration stepsize. In the table below the end points and residence times have been obtained with a stepsize of 1 instead of the default stepsize of 4. For this reduced stepsize the errors in  $z_1$  through  $z_4$  are: 0.44%, 0.8%, 0.56%, and 0.34%, respectively.

The tic-marks in Figure 1.3 indicate increased streamline depth with intervals of 1. It may be verified that these depth markers are consistent with the above calculated streamline depths. Note, that the streamlines reach there maximum depth at the disc rim: no depth markers occur outside the source disc. You will also see this when tracing these streamlines; once a streamline moves outside the disc the  $z$ -value reported above the plot does not change anymore.

### 1.2.3 Residence times

In Figure 1.4 the same problem is depicted as in Figure 1.3, except that the depth markers have been replaced by residence time markers. The residence time  $t$  for a water particle, traveling along a streamline, may be calculated as follows:

$$t - t_0 = \int_0^s \frac{ds}{v_s} \quad (1.12)$$

where  $v_s$  is the average groundwater flow velocity along the streamline. For the case of radial flow in Figure 1.4 we may rewrite the equation as follows:

$$t - t_0 = \int_{r_0}^r \frac{dr}{v_r} \quad (1.13)$$

where  $v_r$  is given by:

$$v_r = \frac{Q_r}{nH} \quad (1.14)$$

and where  $n$  is the aquifer porosity. The groundwater flow discharge  $Q_r$  is calculated differently underneath the source disc than outside the source disc.

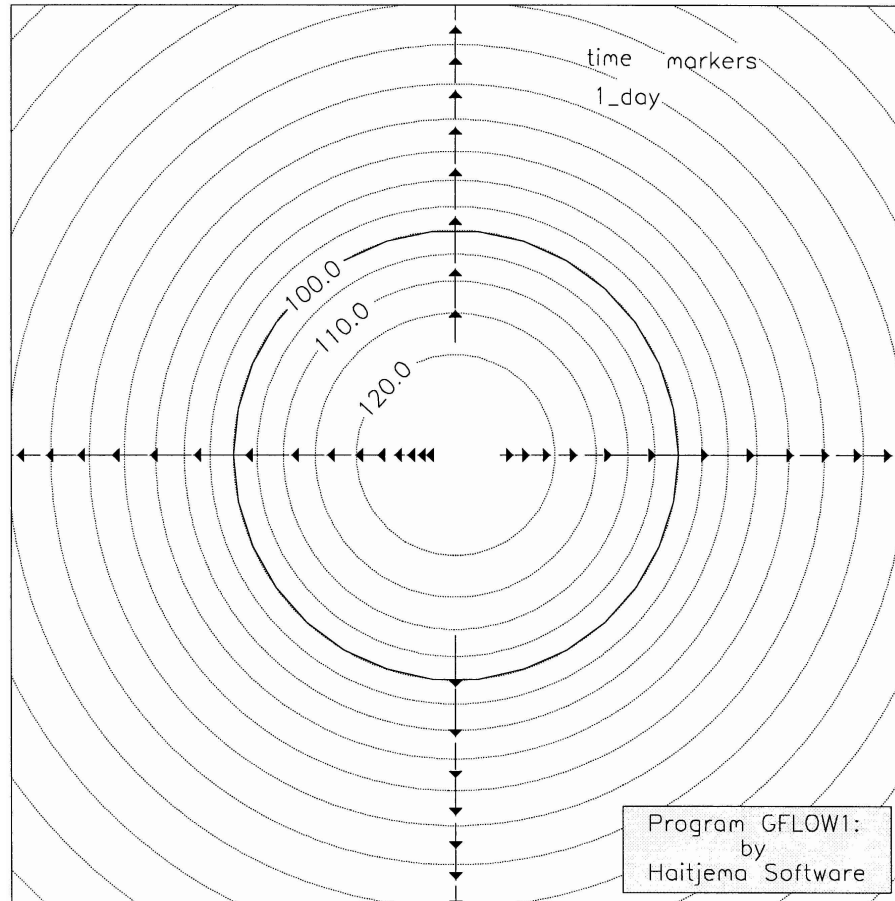


Figure 1.4: Piezometric contours and streamlines with *time* markers for a source disc.



Underneath the source disc we have:

$$Q_r = -\frac{s}{2}r \quad (1.15)$$

while outside the disc:

$$Q_r = \frac{-sR^2}{2} \frac{1}{r} \quad (1.16)$$

Since the streamlines depicted in Figure 1.4 all end outside the disc, we have to break up the integral in (1.13) into two integrals:

$$t - t_0 = \int_{r_0}^R \frac{nH}{-s/2} \frac{1}{r} dr + \int_R^r \frac{nH}{-s/2R^2} r dr \quad (1.17)$$

which yields:

$$t - t_0 = \frac{2nH}{s} \left[ \ln \frac{R}{r_0} + \frac{1}{2} \left( \frac{r^2}{R^2} - 1 \right) \right] \quad (1.18)$$

The starting values  $r_0$  for the four streamlines are: 10, 20, 50, and 80. Substituting the relevant data into (1.18) yields for the residence times  $t_1$  through  $t_4$ , for the four streamlines:

$$\begin{aligned} t_1 &= 4 \left[ \ln \frac{100}{10} + \frac{1}{2} \left( \frac{203.0^2}{100^2} - 1 \right) \right] = 15.45 \\ t_2 &= 4 \left[ \ln \frac{100}{20} + \frac{1}{2} \left( \frac{202.0^2}{100^2} - 1 \right) \right] = 12.5985 \\ t_3 &= 4 \left[ \ln \frac{100}{50} + \frac{1}{2} \left( \frac{201.2^2}{100^2} - 1 \right) \right] = 8.8688 \\ t_4 &= 4 \left[ \ln \frac{100}{80} + \frac{1}{2} \left( \frac{203.7^2}{100^2} - 1 \right) \right] = 7.1913 \end{aligned}$$

The values predicted by GFLOW1, using a stepsize of 4, are (see Table 1.1): 15.47, 12.62, 8.873, and 7.188. The errors are: 0.13%, 0.17%, 0.05%, and 0.05%, respectively. When compared to the residence times obtained from GFLOW1 with a stepsize of 1 (see Table 1.2), the errors are: 1.1%, 1.2%, 0.9%, and 3.4%, respectively.

Observe that the reduced stepsize did not lead to increased accuracy of the residence times, as it did for the streamline depth. Smaller stepsizes will theoretically improve the accuracy of numerical integration procedures, but this increased theoretical accuracy may be offset by machine accuracy limitations. The decrease in stepsize causes an increased number of additions of small numbers to relatively large numbers. GFLOW1 calculations are carried out with only seven (7) significant digits (except for some calculations in the inhomogeneity routines which are carried out in double precision). An optimal stepsize for numerical integration procedures requires a balancing of increased theoretical accuracy and decreased numerical accuracy due to round off errors in the computer. Finally, the stepsize should not be chosen so small that the streamline traces progress too slowly. The default stepsize in the TRACE module of

GFLOW1 is chosen to provide some balance between these conflicting factors, although this may depend on the problem at hand. In case of doubt, the user is advised to experiment with the stepsize and monitor the resulting variations in streamline depth and residence times.

### 1.2.4 Superimposed discs

So far we only tested the implementation of one source disc. In GFLOW1 source or sink discs may be superimposed. In Figure 1.5 five source discs have been superimposed on top of each other. The discharge of each of the discs is -0.2, so that together they have the same discharge as the one disc in Figure 1.3 or Figure 1.4. The data file for this case has been adapted from the original file `valid2.dat` and is printed below:

```
* Written by GFLOW1 version 1.0
error error.log
yes
message nul
echo con
quit
modelorigin      0      0  0
layout
window -200.0000   -200.0000   200.0000   200.0000
quit
title valid2.dat
aquifer
permeability  10.00000
thickness     10.00000
base          0.0000000
porosity      0.2000000
reference     0.0000   100.00000   100.0000
quit
sinkdisc
discharge
*  x    y    xr    yr  top disch.  bottom disch.  label
   0    0   100    0   -0.2        0.0          testdisc1
   0    0   100    0   -0.2        0.0          testdisc2
   0    0   100    0   -0.2        0.0          testdisc3
   0    0   100    0   -0.2        0.0          testdisc4
   0    0   100    0   -0.2        0.0          testdisc5
quit
solve
grid
dotmap off
horizontalpoints 60
go
```

```
quit
switch
error con
message con
echo off
input con
```

The streamline end points and residence times for the case depicted in Figure 1.5 is identical to those reported in Table 1.1. As may be seen by comparing Figure 1.5 to Figure 1.4 or Figure 1.3, the piezometric head distributions are also identical.

The superposition of the discs has been tested by adding identical discs together in order to be able to compare the results with one disc. The chance that GFLOW1 would handle this situation correctly, but different sizes of discs at different locations not, is considered remote.

### 1.2.5 Top and bottom strengths

Discharge specified sink discs in GFLOW1 may be given a strength at the top of the aquifer (done in the above examples), a strength at the bottom of the aquifer, or both.

In Figure 1.6 a source disc is displayed with a top and bottom recharge rate of  $s = -0.5$ . Together these recharge rates provide the same total strength as for the earlier tested disc with only a top recharge rate ( $s = -1$ ). The data file for this case has been adapted from `valid2.dat` and is listed below:

```
* Written by GFLOW1 version 1.0
error error.log
yes
message nul
echo con
quit
modelorigin      0      0  0
layout
window -200.0000   -200.0000   200.0000   200.0000
quit
title valid2.dat
aquifer
permeability    10.00000
thickness       10.00000
base            0.0000000
porosity        0.2000000
reference       0.0000   100.00000   100.0000
quit
sinkdisc
discharge
* x  y  xr  yr top disch. bottom disch. label
```

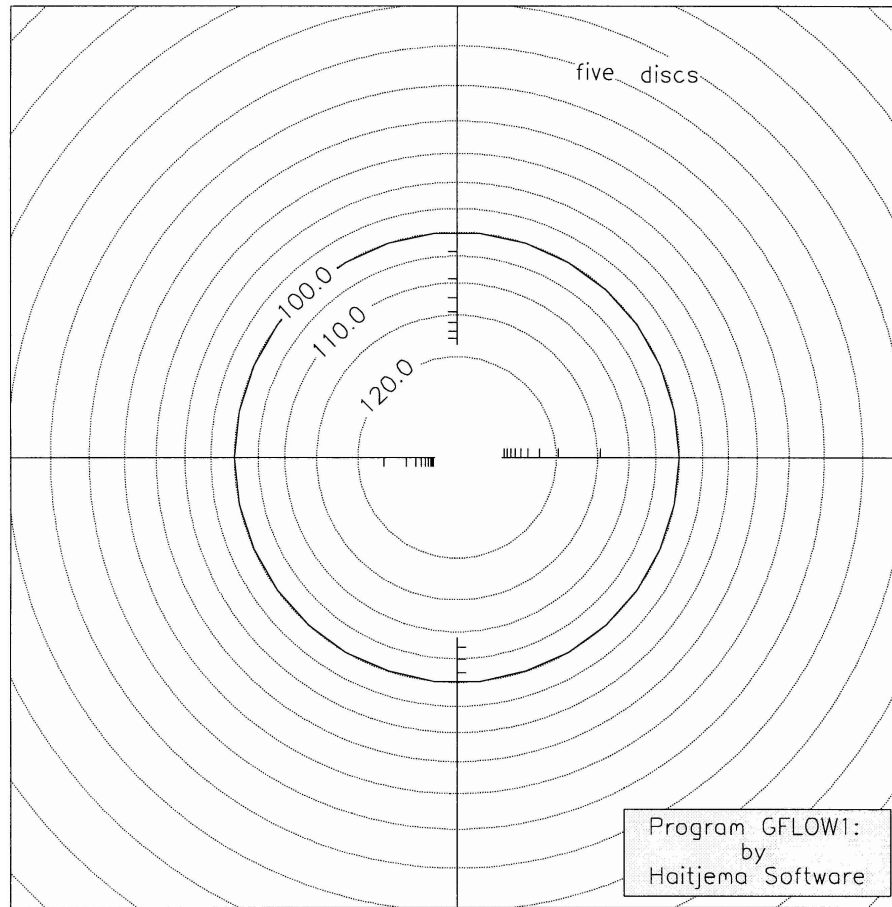


Figure 1.5: Piezometric contours and streamlines with *depth* markers for five source discs on top of each other and a combined recharge rate equal to the one disc tested before.

Table 1.3: Streamlines and residence times for top/bottom recharge

starting x,y,z	end x,y,z	residence time
-10 ; + 0 ; +10	-201.2 ; +0.000 ; +5.060	15.32
+20 ; + 0 ; +10	-203.5 ; +0.000 ; +5.203	12.72
+0 ; +50 ; +10	+0.000 ; +201.8 ; +6.261	8.918
+0 ; -80 ; +10	+0.000 ; -203.9 ; +8.078	7.208

```

0 0 100 0 -0.5      -0.5      testdisctopbot
quit
solve
grid
dotmap off
horizontalpoints 60
go
quit
switch
error con
message con
echo off
input con

```

The same streamlines have been traced as for the previous cases. However, the streamline depth is now affected by the different distribution of the recharge. Due to the symmetric bottom and top infiltration rates the streamlines started from the aquifer top do not descend below the midpoint in the aquifer: they stay above elevation 5. In Table 1.3 the streamline starting points, end points, and residence times are given for the case depicted in Figure 1.6. Because of the different three-dimensional paths of the streamlines in Figure 1.6 the streamline tracing routine in GFLOW1 terminates the streamlines at slightly different points, which explains the small differences between the residence times in Table 1.1 and Table 1.3.

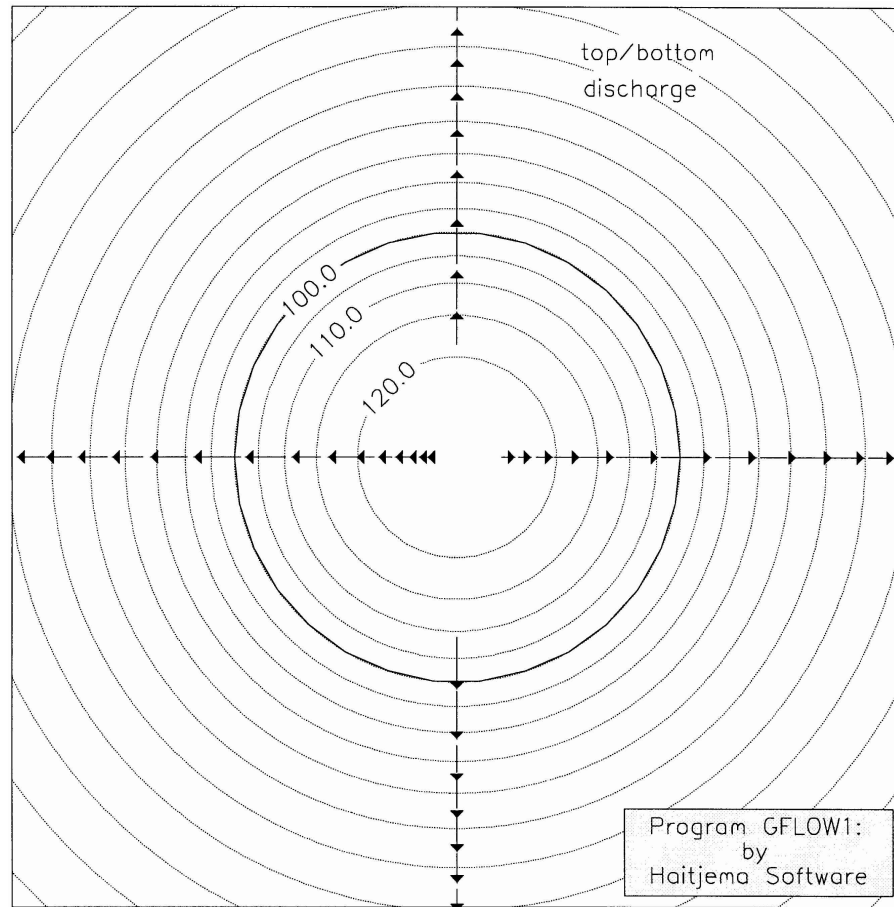


Figure 1.6: Piezometric contours and streamlines with *time* markers for a source discs with the same top and bottom recharge rate which together is equal to the recharge rate of the single disc tested before.

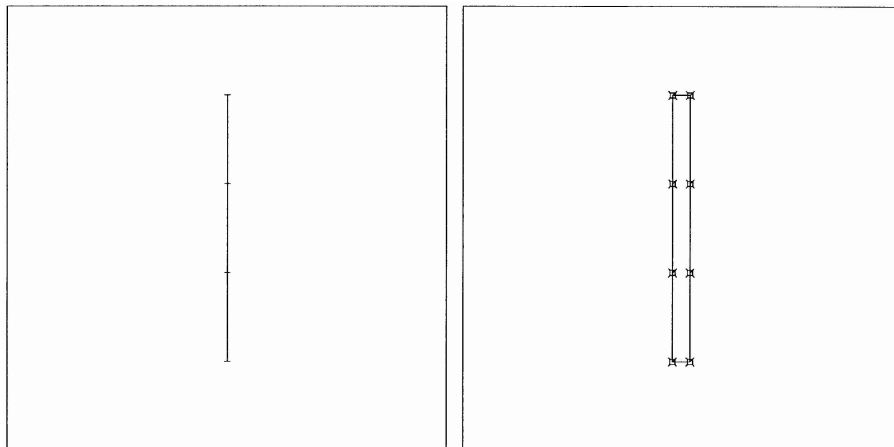


Figure 1.7: Three line sinks with strength of  $-0.4$  (left) and a recharge area (inhomogeneity) with strength  $-0.1$  (right). Both features have a width of 4.

### 1.3 LINE SINK

Strings of line sinks with constant strength are used in GFLOW1 to represent head specified boundaries (Dirichlet boundary conditions) or head dependent flow boundaries (Cauchy boundary conditions). Strack and Haitjema (1981) demonstrated the suitability of line sink strings to approximate streams and lake boundaries by using a line sink string to approximate an equipotential boundary near a well. In this section we will investigate the *implementation* of the line sink function in GFLOW1.

In Figure 1.7 the layout of a string of three line sinks (left-hand figure) is shown together with the layout of a recharge inhomogeneity (right-hand figure). Both the line sink string and the recharge area infiltrate the same amount of water, evenly distributed over the line and rectangle in Figure 1.7. The line sinks have a width of 4 and are discharge specified. Listings of the data file with the line sinks, `valid3a.dat`, and with the recharge inhomogeneity, `valid3b.dat`, follow below.

The file `valid3a.dat`:

```
* Written by GFLOW1 version 1.0
error error.log
yes
message nul
echo con
quit
modelorigin          0          0  0
layout
wind -50 -50 50 50
```

```

quit
title valid3a
aquifer
permeability 10.00000
thickness 10.00000
base 0.0000000
porosity 0.2000000
reference 100.0000 0.0000000 50.00000
uniflow 0.70710678 0.70710678
quit
linesink
discharge
* x1 y1 x2 y2 exf. rate width label
  0. -30. 0. -10. -0.4000 4.000 linesink1
  0. -10. 0. 10. -0.4000 4.000 linesink2
  0. 10. 0. 30. -0.4000 4.000 linesink3
quit
switch
error con
message con
echo off
input con

```

The file valid3b.dat:

```

* Written by GFLOW1 version 1.0
error error.log
yes
message nul
echo con
quit
modelorigin 0 0 0
layout
wind -50 -50 50 50
quit
title valid3b
aquifer
permeability 10.00000
thickness 10.00000
base 0.0000000
porosity 0.2000000
reference 100.0000 0.0000000 50.00000
uniflow 0.70710678 0.70710678
quit
inhom
inhom 10 -0.1 0.2
-2 -30

```



```

2 -30
2 -10
2 10
2 30
-2 30
-2 10
-2 -10
quit
switch
error con
message con
echo off
input con

```

Both the line sink string and the recharge inhomogeneity are located in a uniform flow field of strength 1 that flows under 45 degrees from the lower left of the domain to the upper right.

In GFLOW1 line sinks with a specified width are used to represent streams with that same width. The width of the line sink is used to calculate the line sink strength for head dependent flow boundaries. An alternative way to represent a stream is to use sink or source distributions over quadrilaterals with which the stream width is modeled explicitly, e.g. as done in SLAEM<sup>1</sup> with so-called areal elements.

### Heads near line sink string and recharge inhomogeneity

In Figure 1.8 piezometric contours are plotted for both line sink string and the recharge inhomogeneity in Figure 1.7. The piezometric contours are plotted on top of each other and do not noticeably differ; only single contour lines are visible in Figure 1.8. In Figure 1.9 a close-up of the domain in Figure 1.8 is presented. On this scale some differences are visible in the immediate vicinity of the line sinks or recharge inhomogeneity. The contour levels are plotted on the contours for the recharge inhomogeneity.

### Streamline depth change

When a streamline crosses the line sink string or the recharge inhomogeneity a change in streamline depth must occur due to the water added at the top of the aquifer. Note, the line sink or line source is interpreted as removing or adding water *at the top of the aquifer*. The total infiltration of both features in Figure 1.7 is  $0.4 [L^2/T]$ . The discharges just to the left and to the right of the line sink string, calculated by GFLOW1, are reported in Table 1.4. The discharge component  $Q_y$  is parallel to the line sink and does not change. However, the discharge component  $Q_x$ , which is normal to the line link, jumps by 0.3999915, which is as close to 0.4 as the machine accuracy will allow.

---

<sup>1</sup>Trademark of Strack Consulting, Inc.

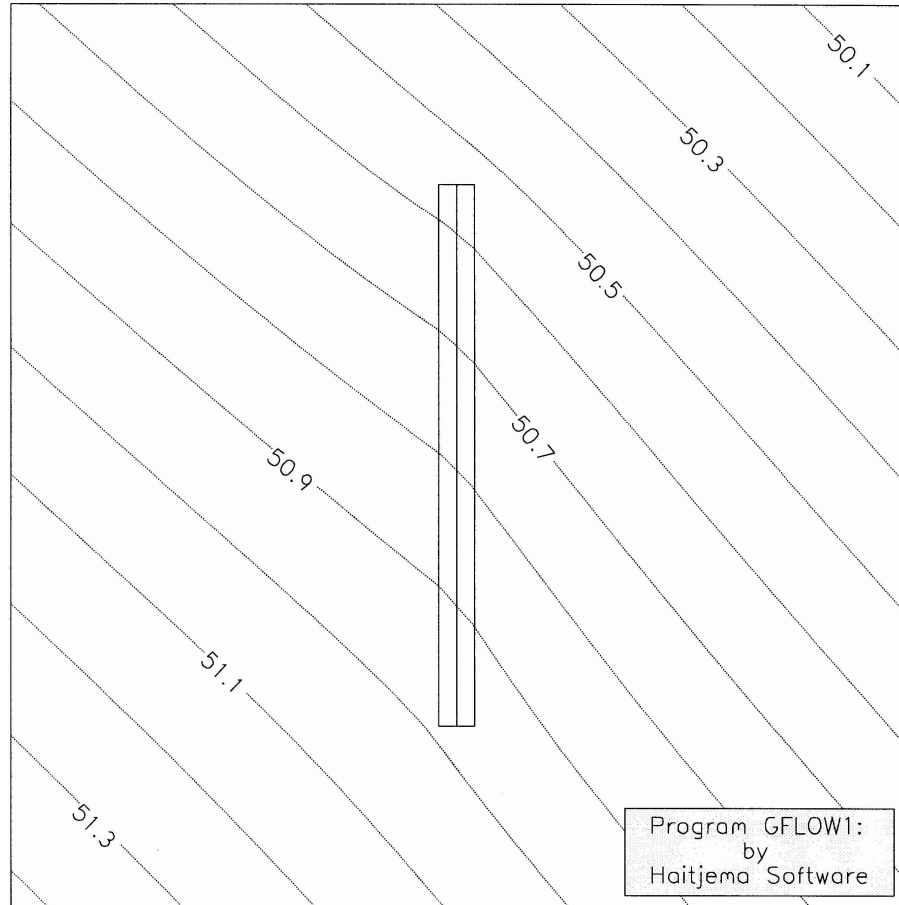


Figure 1.8: Piezometric contours for the line sinks and recharge inhomogeneity are indistinguishable on this scale.

Table 1.4: Discharges to the left and the right of the line sink string

x,y,z	$Q_x = Q_n$	$Q_y$
-0.001 ; 0 ; +10	0.5071110	0.7071068
+0.001 ; 0 ; +10	0.9071025	0.7071068

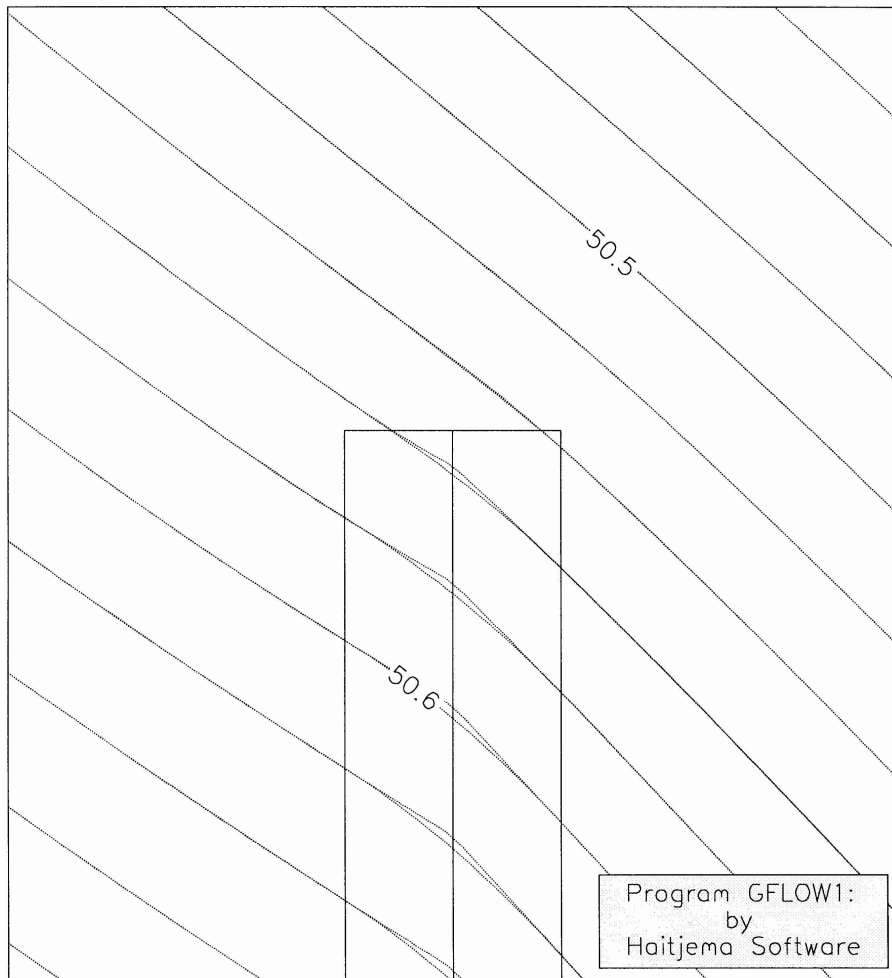


Figure 1.9: Some differences in contours for a close-up of the line sink string and recharge inhomogeneity.

Table 1.5: Comparison of computed and specified heads and strengths for the line sinks in `valid3a.dat` and `valid3c.dat`.

center	calc./spec. head	spec. strength	calc. strength
0 ; -20	50.92400	-0.40000	-0.3999080
0 ; 0	50.79185	-0.40000	-0.4000699
0 ; -20	50.64116	-0.40000	-0.3999080

The streamline depth  $z^-$  to the left of the line sink string will increase to the depth  $z^+$  as given by:

$$\frac{z^+}{z^-} = \frac{Q_n^+}{Q_n^-} \quad (1.19)$$

where  $Q_n^+$  and  $Q_n^-$  are the normal discharges ( $Q_x$  in this case) to the left and the right of the line sink, respectively. Consequently, with reference to Table 1.4,

$$z^+ = \frac{0.5071110}{0.9071025} z^- = 0.55904487 z^-$$

When starting a streamline to the left of the line sink string at the aquifer top ( $z^- = 10.0$ ) the streamline depth to the right of the line sink string becomes: 5.5905. Starting a streamline at the point  $(-2.0; -2.0; 10)$  in GFLOW1, for the solution to `valid3a.dat`, results in a streamline depth  $z^+ = 5.591$ , which is the exact value rounded to three decimals. When starting at the same point for the case of the recharge inhomogeneity, the streamline depth  $z^+$  to the right of the recharge inhomogeneity depends on the stepsize in trace! For stepsizes of 1, 0.1, and 0.02, the resulting values of  $z^+$  are: 5.484, 5.614, and 5.598, respectively. The smaller the stepsize, the more accurate the streamline depth, until the machine accuracy is exceeded.

The streamline depth change for the line sink is calculated by GFLOW1 by use of (1.19), while the streamline depth change underneath the recharge inhomogeneity is calculated by numerically integrating the vertical velocity  $v_3$ . Consequently, a relatively small stepsize is required to obtain accurate results for the latter computation. In view of this, small stepsizes should be used when tracing streamlines underneath narrow recharge inhomogeneities. In most practical cases, however, the recharge inhomogeneities will be wide as compared to the stepsize, leading to reasonably accurate streamline depth calculations.

### Head specified line sinks

The line sinks in `valid3a.dat` are strength specified and create heads at the line sink centers as reported in Table 1.5. These heads are use in the file `valid3c.dat` to create *head specified* line sinks. After switching in `valid3c.dat` and solving, GFLOW1 reports the strenghts listed in the most right-hand column in Table 1.5. The strengths are within the machine accuracy of those

specified in `valid3a.dat`, demonstrating the integrity of the head specified line sink implementation in GFLOW1. Note, the calculated strengths have been obtained by use of the cursor option in the line sink module (pointing at the line sink and pressing `< Enter >`).

## 1.4 INHOMOGENEITY DOMAINS

The suitability of line doublet strings to represent domains of different hydraulic conductivity has been demonstrated by Strack and Haitjema (1981) who compared the exact solution for a circular inhomogeneity to a circular (regular) polygon of line doublets. The same type of comparison is repeated in this section to verify the proper implementation of the line doublet strings in GFLOW1.

Note, the exact solution was temporarily programmed into GFLOW1, but is not available in the educational or commercial version of the program. To allow future comparisons, the contour plots for the exact solution are provided in the directory `\GFLOW\VALID` as PostScript files: `valid4a.pst`, `valid4b.pst`, and `valid4c.pst`. These files contain the exact contours for the GFLOW1 representations, using line doublet strings, as defined in the input data files `valid4a.dat`, `valid4b.dat`, and `valid4c.dat`, respectively.

### 1.4.1 Discontinuity in hydraulic conductivity

In Figure 1.10 the piezometric contours are plotted for a circular inhomogeneity in a uniform flow field, see Strack (1989). The inside hydraulic conductivity is 1, while the outside conductivity is 10. The uniform flow rate is 1 and the head at the center of the circle is 100. In Figure 1.11 the exact solution of Figure 1.10 has been superimposed onto a GFLOW1 solution to a inhomogeneity domain in the same uniform flow field. The inhomogeneity domain approximates the circular domain in Figure 1.10 by use of 12 line doublets. The contours produced by GFLOW1 have not been labeled, but are seen to be close to the exact solution. The GFLOW1 problem for this case is defined in the file `valid4a.dat` which is printed below.

```
* Written by GFLOW1 version 1.0
error error.log
yes
message nul
echo con
quit
modelorigin      0          0  0
title valid4a
layout
window -20.00000   -20.00000   20.00000   20.00000
quit
aquifer
permeability 10.000000
```

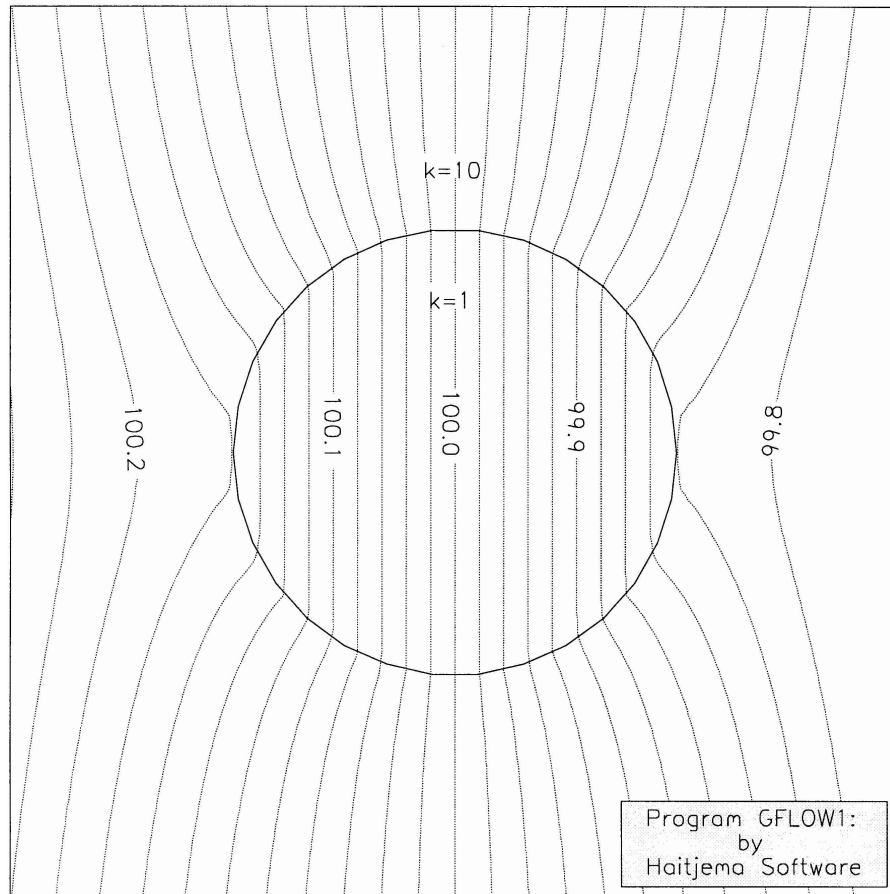


Figure 1.10: Exact solution for a circular inhomogeneity in a uniform flow field. The inside and outside conductivity are 1 and 10, respectively.

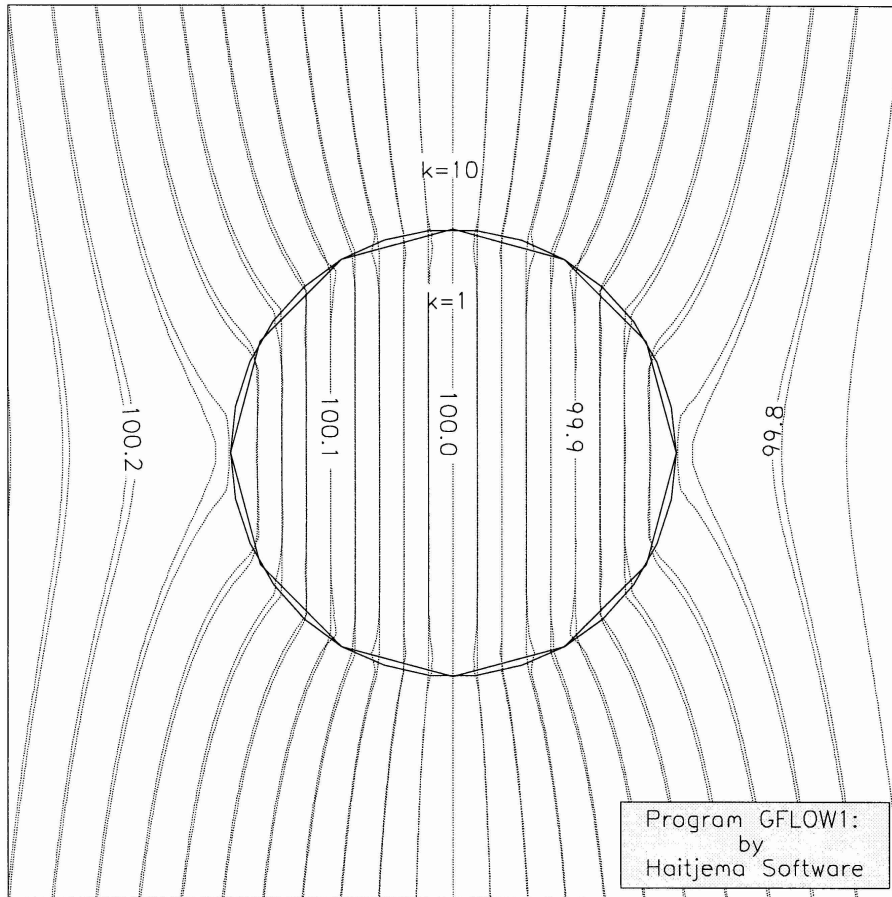


Figure 1.11: GFLOW1 solution for 12 line doublets superimposed onto the exact solution. The inside and outside conductivity are 1 and 10, respectively.

```

thickness      10.00000
base           0.0000000
porosity       0.2000000
uniflow 1 0
reference      0.0000000      0.0000000      100.0000
quit
inhomogeneity
*      hydraul. cond.   added exf.rate   porosity
inhom      1.000000      0.000000      0.1000000
0 10
5 8.66
8.66 5
10 0
8.66 -5
5 -8.66
0 -10
-5 -8.66
-8.66 -5
-10 0
-8.66 5
-5 8.66
quit
switch
error con
message con
echo off
input con

```

In Figure 1.12 the same exact solution as in Figure 1.10 is shown, except the outside hydraulic conductivity is reduced from 10 to 0.1. In Figure 1.13 a GFLOW1 solution, again using 12 line doublets has been superimposed onto the exact solution in Figure 1.12. The GFLOW1 problem for this case is defined in the file `valid4b.dat`, which is printed below.

```

* Written by GFLOW1 version 1.0
error error.log
yes
message nul
echo con
quit
modelorigin      0      0 0
title valid4b
layout
window -20.00000      -20.00000      20.00000      20.00000
quit
aquifer
permeability 0.1000000

```



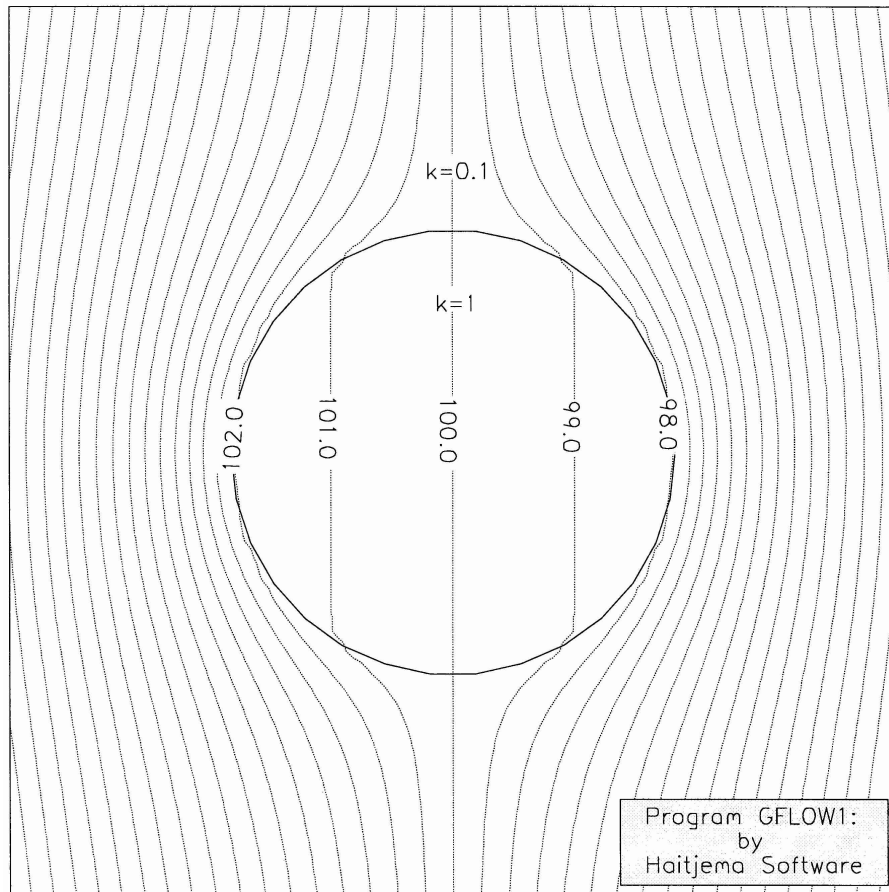


Figure 1.12: Exact solution for a circular inhomogeneity in a uniform flow field. The inside and outside conductivity are 1 and 0.1, respectively.

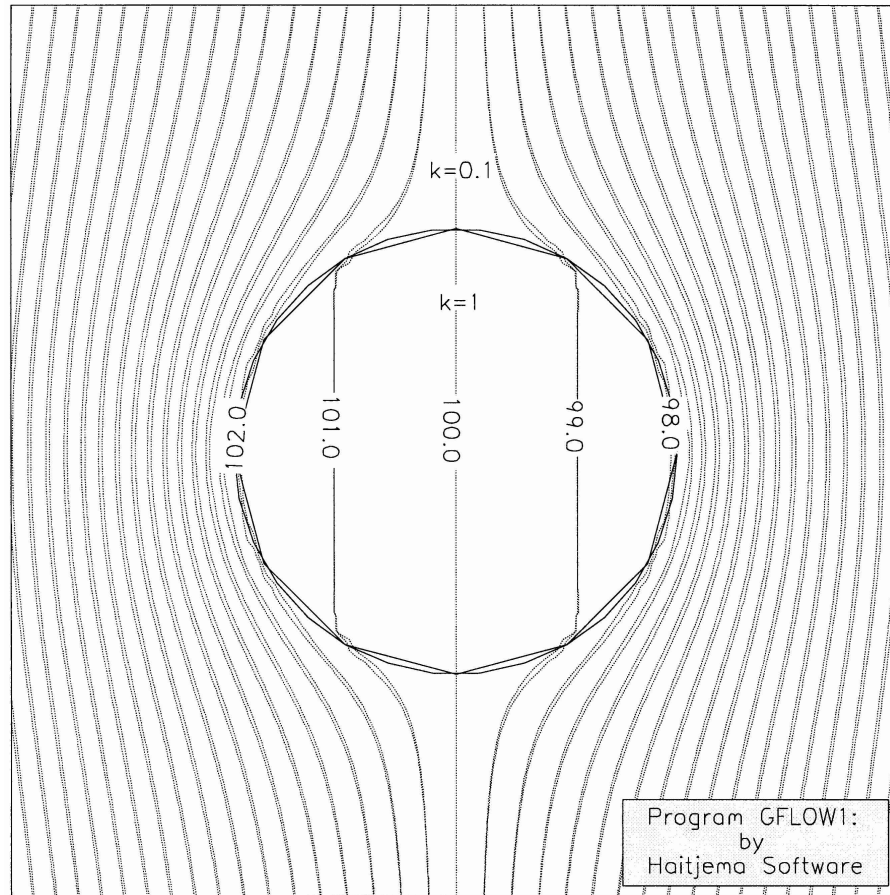


Figure 1.13: GFLOW1 solution for 12 line doublets superimposed onto the exact solution. The inside and outside conductivity are 1 and 0.1, respectively.

```

thickness      10.00000
base           0.0000000
porosity       0.2000000
uniflow 1 0
reference      0.0000000      0.0000000      100.0000
quit
inhomogeneity
*      hydraul. cond.      added exf.rate      porosity
inhom      1.000000      0.000000      0.1000000
0 10
5 8.66
8.66 5
10 0
8.66 -5
5 -8.66
0 -10
-5 -8.66
-8.66 -5
-10 0
-8.66 5
-5 8.66
quit
switch
error con
message con
echo off
input con

```

The results presented in Figure 1.11 and Figure 1.13 may be improved upon by better approximating the circle by a regular line doublet polygon. The current polygon has its vertices on the circle and its sides inside the circle. A better approximation would be obtained when selecting a slightly larger polygon to make the surface area of the polygon equal to that of the circle, compare also Figure 1.15 and Figure 1.16 in the next section. Of course, an other way of improving the approximation is to simply increase the number of line doublets in the polygon.

### 1.4.2 Discontinuity in recharge

GFLOW1 allows the user to specify an “added exfiltration rate” for an inhomogeneity domain. To test the implementation of this feature a comparison is made to the exact solution for a circular inhomogeneity with a source disc on top of it. In Figure 1.14 the piezometric contours are presented for the case of Figure 1.12 with a sink disc of strength  $-0.1$  (source disc) on top of the circular inhomogeneity. In Figure 1.15 a GFLOW1 solution has been superimposed onto the exact solution presented in Figure 1.14. The GFLOW1 problem for

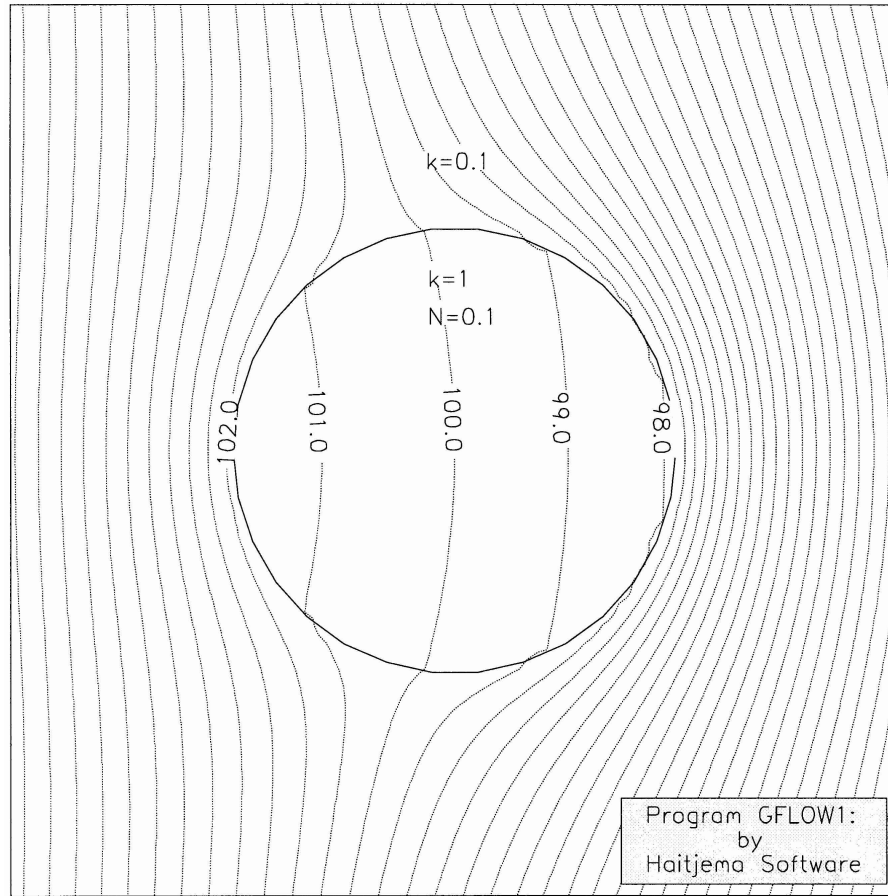


Figure 1.14: Exact solution for a circular inhomogeneity with a recharge rate of 0.1 (inside the circle). The inside and outside conductivity are 1 and 0.1, respectively.

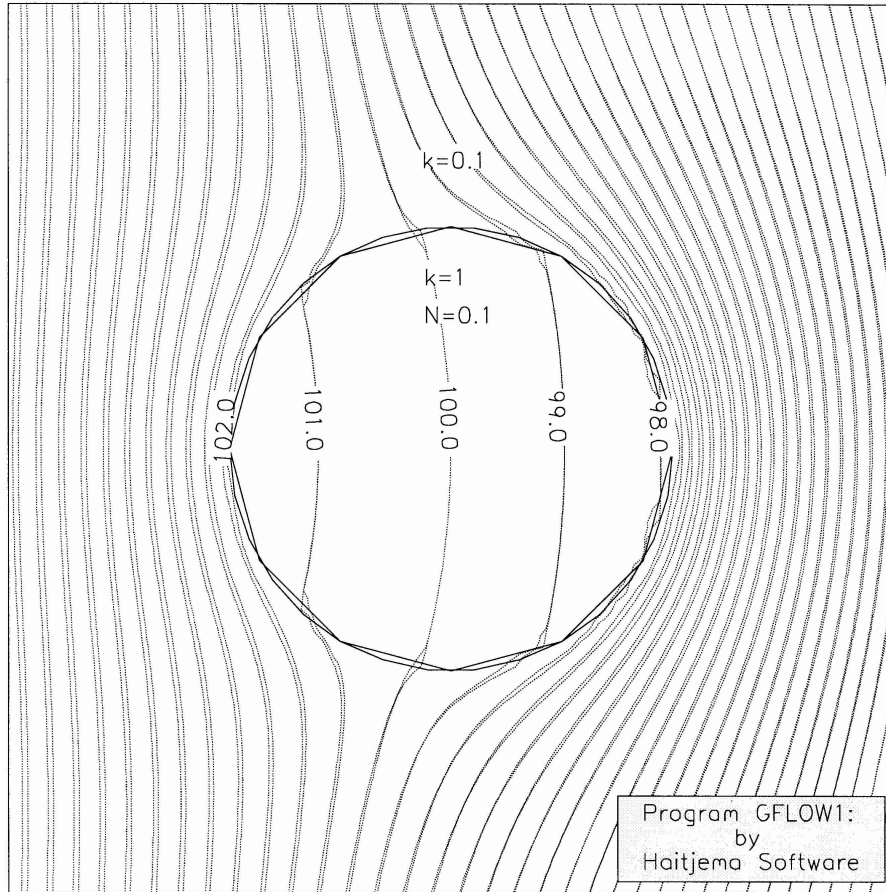


Figure 1.15: GFLOW1 solution for 12 line doublets superimposed onto the exact solution. The “added exfiltration rate” of the inhomogeneity in GFLOW1 is  $-0.1$ . The inside and outside conductivity are 1 and 0.1, respectively.

this case is defined in the file `valid4c.dat` which is printed below.

```
* Written by GFLOW1 version 1.0
error error.log
yes
message nul
echo con
quit
modelorigin          0          0  0
title valid4c
layout
window -20.00000      -20.00000      20.00000      20.00000
quit
aquifer
permeability 0.1000000
thickness     10.00000
base          0.0000000
porosity      0.2000000
uniflow 1 0
reference      0.0000000      0.0000000      100.0000
quit
inhomogeneity
*          hydraul. cond.    added exf.rate    porosity
inhom      1.000000      -0.1000000      0.1000000
0 10
5 8.66
8.66 5
10 0
8.66 -5
5 -8.66
0 -10
-5 -8.66
-8.66 -5
-10 0
-8.66 5
-5 8.66
quit
switch
error con
message con
echo off
input con
```

The contours in Figure 1.15 do not match too well! This is partly due to the fact that the line doublet polygon fits inside the circle of radius 10. Consequently, the inhomogeneity domain has a smaller surface area, and thus infiltrates less water, than the circular area in the exact solution. In file `valid4cc` the line

doublet polygon has been changed to include the exact same area as the circle in Figure 1.14. The piezometric contours generated by GFLOW1 for this case are superimposed onto the exact solution, see Figure 1.16. Now a much better match is obtained! The data file `valid4cc.dat` is printed below.

```
* Written by GFLOW1 version 1.0
error error.log
yes
message nul
echo con
quit
modelorigin      0      0  0
title valid4cc
layout
window -20.00000   -20.00000   20.00000   20.00000
quit
aquifer
permeability  0.1000000
thickness     10.00000
base          0.0000000
porosity      0.2000000
uniflow 1 0
reference     0.0000000   0.0000000   100.0000
quit
inhomogeneity
*      hydraul. cond.   added exf.rate   porosity
inhom   1.000000    -0.1000000    0.1000000
0 10.233267
5.11663354 8.86226925
8.86226925 5.11663354
10.233267 0
8.86226925 -5.11663354
5.11663354 -8.86226925
0 -10.233267
-5.11663354 -8.86226925
-8.86226925 -5.11663354
-10.233267 0
-8.86226925 5.11663354
-5.11663354 8.86226925
quit
switch
error con
message con
echo off
input con
```

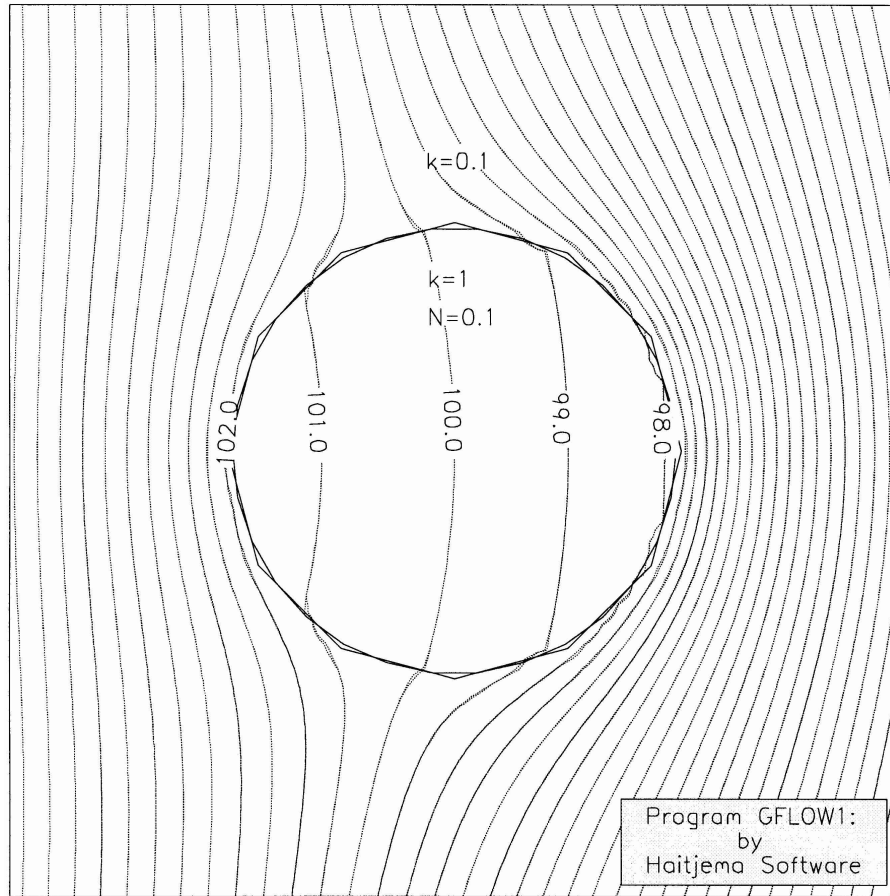


Figure 1.16: GFLOW1 solution for 12 line doublets superimposed onto the exact solution. The polygon has been enlarged to obtain the same surface area (thus same infiltration) as for the circle. The inside and outside conductivity are 1 and 0.1, respectively.



### 1.4.3 Discontinuity in porosity

To verify the implementation of porosity differences in inhomogeneity domains, a streamline is traced across the inhomogeneity in Figure 1.14, both for the case that the inside porosity is 0.1, see `valid4c.dat`, and for the case that the inside porosity equals the outside porosity: 0.2. The residence times reported by GFLOW1, using a stepsize of 0.1, are: 11.09 and 22.12, respectively. Indeed, the groundwater velocity has increased by a factor 2 (the value of 22.12 instead of 22.18 may be attributed to the inaccuracy of the numerical integration procedure in GFLOW1).

### 1.4.4 Residence times

GFLOW1's residence time calculations for streamlines which intersect inhomogeneity domains are verified by comparison of the total residence time for a streamline through the center of the inhomogeneity in Figure 1.12 with an exact solution. The residence time is given by (1.4):

$$t = \int_{x_0}^x \frac{nHdx}{Q_x} \quad (1.20)$$

where  $Q_x$  outside the circular domain, along the  $x$ -axis, is given by,

$$Q_x = Q_0 \left( 1 - \frac{k - k_1}{k + k_1} \frac{R^2}{x^2} \right) \quad (x^2 \geq R^2) \quad (1.21)$$

and inside the domain by:

$$Q_x = Q_0 \frac{2k_1}{k + k_1} \quad (x^2 \leq R^2) \quad (1.22)$$

This results in the following integrals for the residence time from the point  $(-20; 0)$  to  $(+20; 0)$ :

$$t = \frac{nH}{Q_0} \left( \int_{-20}^{-10} \frac{x^2 dx}{x^2 + a^2} + \frac{k + k_1}{2k_1} \int_{-10}^{+10} dx + \int_{+10}^{+20} \frac{x^2 dx}{x^2 + a^2} \right) \quad (1.23)$$

where  $a^2$  is defined as:

$$a^2 = -\frac{k - k_1}{k + k_1} R^2 = \frac{k_1 - k}{k_1 + k} R^2 \quad (1.24)$$

The first integral in (1.23) becomes:

$$\int_{-20}^{-10} \frac{x^2 dx}{x^2 + a^2} = \left[ x - a \arctan \frac{x}{a} \right]_{-20}^{-10}$$

or with the data contained in `valid4b.dat`:

$$-10 - 9.045340337 \arctan \frac{-20}{9.045340337} +$$

Table 1.6: Residence times for a streamline starting at  $(-20; 0)$  and moving across the inhomogeneity defined in the file `valid4b.dat`.

residence time	stepsize	end point
50.64	0.4	20.40 ; 0
50.15	0.2	20.00 ; 0
50.22	0.1	20.00 ; 0
50.34	0.05	20.05 ; 0

$$- \left( -20 - 9.045340337 \arctan \frac{-10}{9.045340337} \right)$$

or

$$10 - 9.045340337(1.14605875 - 0.835481324) = 7.19072$$

The last integral in (1.23) yields the same result. Substituting all relevant data in (1.23) yields:

$$2(7.19072 + 11 + 7.19072) = 50.76$$

When tracing streamlines in GFLOW1 for the problem defined by `valid4b.dat` the following residence times are reported, see Table 1.6. The inaccuracies in the residence time may be attributed to two different factors: (1) the numerical integration procedure in GFLOW1, and (2) the approximate manner in which the twelve line doublets model the circular inhomogeneity.

## **1.5 COMPARING LINE SINKS WITH AREAL ELEMENTS**

*Under development.*

*Results on file with Haitjema Software LLC*

## **1.6 STREAM FLOW ACCUMULATION**

*Under development.*

*Results on file with Haitjema Software LLC*

## **1.7 STREAM FLOW VARIATIONS DUE TO A NEARBY WELL**

*Under development.*

*Results on file with Haitjema Software LLC*

## **1.8 CONJUNCTIVE SURFACE WATER / GROUNDWATER SOLUTIONS**

*Under development.*

*Results on file with Haitjema Software LLC*